

# Performance of Carbon Nanosheet Electrode from Aquatic Wood Waste in Supercapacitor

Sri Haryati<sup>a,\*</sup>, Djoni Bustan<sup>a</sup>, Nirwan Syarif<sup>b</sup>, Chew Tin Lee<sup>c</sup>

<sup>a</sup>Department of Chemical Engineering, Universitas Sriwijaya, Inderalaya Sumsel 30662, Indonesia

<sup>b</sup>Department of Chemistry, Universitas Sriwijaya, Inderalaya Sumsel 30662, Indonesia

<sup>c</sup>Department of Bioprocess and Polymer Engineering, School of Chemical and Energy Engineering, Universiti Teknologi

Malaysia, Johor, Malaysia

[haryati\\_djoni@yahoo.co.id](mailto:haryati_djoni@yahoo.co.id)

Disposal of conventional polymer-based electrodes and capacitor can cause pollutions or incur high cost. More carbon based nanosheet electrode is more environmental friendly. Novel supercapacitors were fabricated using carbon nanosheet electrode. Two pieces of thick layer carbon nanosheet electrodes were used as the cathode; the anode were made of carbon nanosheet and graphite mixture with a ratio of 7: 3, 10 % binder and coated on top of a glass surface. The polymer gel electrolytes containing barium carbonate (BaCO<sub>3</sub>) or calcium carbonate (CaCO<sub>3</sub>) were filled in the middle of the electrodes to act as a supercapacitor. The concentrations of electrolytes, BaCO<sub>3</sub> and CaCO<sub>3</sub> were 10 %; 20 %; 30 %. The performance of the supercapacitors was determined by cyclic voltammetry, and charge-discharge galvanostatic methods performed using a potentiostat. The decreasing in capacitances occurred along with the increase of scan rate, from 5 mV s<sup>-1</sup> to 100 mV s<sup>-1</sup>. There is only a slight decrease in the first cycle, as shown by the increased slope of 20 % CaCO<sub>3</sub> of supercapacitor. The first cycle plot shows the existence of linearity both in the direction of charging and discharging. All supercapacitors have the same slope value indicating the same rate for both charging and discharging process. Except for the supercapacitor with 20 % CaCO<sub>3</sub> where different slope values were observed for its charging and discharging rate, i.e., 1.345 and -1.344. The result showed that the supercapacitor has a charging rate faster than its discharging rate. The cyclic voltammetry tests showed that the highest value of 6.95 mF g<sup>-1</sup> was achieved using the supercapacitor of 10 % CaCO<sub>3</sub> as electrolyte; or 3.91 mF g<sup>-1</sup> with 10 % BaCO<sub>3</sub>. A novel supercapacitor, using carbon nanosheets derived from aquatic wood waste as electrodes and polymer-based gel as electrolytes, was developed.

## 1. Introduction

The conventional industry uses polymer-based materials to fabricate electrodes and capacitors. Their disposal cause pollutions or incur high cost of waste treatment. The demand for clean and sustainable material resources for electrode is increasing (Fic et al., 2018). Carbonaceous materials, derived from wood waste thermal treatment such as pyrolysis, should be promoted as a greener substitute for polymer-based carbon electrodes. Wood wastes could be converted into a range of carbonized products such as char or activated carbon following the pyrolysis process. The carbonized products can be classified as a sustainable energy material (Correa and Kruse, 2018). Carbon material embodies non-heavy metal and no-excessive substance in its bulk (Paola Giudicianni et al., 2017) and will not harm soil when it is disposed to ground.

Through the innovative pyrolysis (Syarif and Pardede, 2014), wood waste can be converted as a carbon nanosheet with high surface area properties and used as electrodes with good electrochemical. This study evaluates the performance of supercapacitors made from the novel carbon nanosheet, a carbonized pyrolyzation aquatic wood waste. The morphology of this material has been reported by Syabania et al. (2018). Syarif and Prasagi (2016) reported the electrochemical properties of this carbon nanosheet to be applicable as a supercapacitor. This paper further characterized this carbon nanosheet as a supercapacitor. The performances of the supercapacitors were evaluated using cyclic voltammetry and galvanostatic charging-discharging instrumentations.

## 2. Materials and methods

### 2.1 Supercapacitor preparation

Electrodes for supercapacitor were made by mixing the carbon and graphite at a ratio 7:3 using 10 % w/w of polyaniline as binder to form the paste. The paste was smeared into a piece of glass. A spatula was used to spread the paste evenly and to make the layer thin and more conductive. A thin layer of carbon electrode with the adhesive surface was formed. Exfoliated carbon granules were laid on the adhesive surface to make the surface a shiny plate. Layering was repeated many times to achieve a good of conductivity ( $> 0.01 \text{ Scm}^{-1}$ ) (Lekawa-Raus et al., 2014). The thin-layered carbon nanosheet formed was used as the electrode to be fabricated as a supercapacitor when the resistance reaches a minimum level ( $\sim 10\text{-}100 \text{ ohm}$ ). The electrodes with the size of 190 mm (L) x 30 mm (W) x 1 mm (T) were formed and used as the cathode and anode. Figure 1 shows the diagram of the carbon nanosheets. The middle part of the supercapacitor (electrolyte, Figure1) used polymer – based electrolytes made of 10 – 30 % barium carbonate ( $\text{BaCO}_3$ ) or calcium carbonate ( $\text{CaCO}_3$ ) and polyvinyl alcohol (PVA). The mixture formed a gel consistency and solidified after drying. A plastic clamp was arranged to stick together the cathode, electrolyte and anode as shown in Figure 1. The thin-layered carbon nanosheet electrode is dried for 3 h in a desiccator and ready to be used as a supercapacitor. Capacitances were tested using the cyclic voltammetry and galvanostatic for charging and discharging.

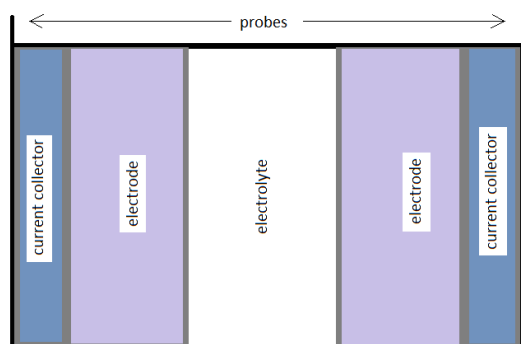


Figure 1: Schematic illustration of a supercapacitor

### 2.2 Supercapacitor performance test

The performance of the supercapacitors is measured in capacitance (Iro et al., 2016) as measured using the cyclic voltammetry test or voltammogram (Allagui et al., 2016). Measurement was conducted using a potentiostat (Autolab). The relationship between the capacitance and voltammogram is given by Eq(1).

$$C_{avg} = \frac{\Delta Q}{(s \times \Delta V)} = \frac{(\int IdV)}{(s \times \Delta V \times w)} \quad (1)$$

The capacitance value is ( $C_{avg}$ ); Q is the total charges, which has been accumulated with the potential window ( $\Delta V$ ) and W is weight of carbon mass on electrode; I is the current flows between anodic and cathode; S is the potential scan rate applied by the potentiostat.  $\int IdV$  is the integral of voltammogram, obtained graphically as the area under the curve. The supercapacitor (Fig. 1) has two electrodes. These electrodes was initialized by connecting the reference and counter probes of potentiostat to the anode and the working probe to the cathode. The concentration of electrolytes,  $\text{BaCO}_3$  or  $\text{CaCO}_3$  were 10 %; 20 %; 30 %. The tests were done by varying the scan rate, i.e., 5, 10, 20, 40, 60, 100  $\text{mV s}^{-1}$ .

The galvanostatic charging-discharging measurement employed the function generator, oscilloscope and resistor to test the charging-discharging cycles of the supercapacitors (Zhi et al., 2018). Voltage readings were provided by channel 1 and 2 of the oscilloscope. Supercapacitor undergoes charging through a resistor without using a switch. A function generator carried out charging-discharging with a voltage applied by both probes of the generator. The square wave function applied in the highest voltage was used as the charging voltage and the lowest voltage was used as the discharge voltage. Channel 1 on the oscilloscope is used to monitor the voltage supplied by the wave function whereby a process of switching between charging and discharging of charge occurs. Channel 2 is used to record the charging and discharging of the supercapacitor. The charge-discharge cycle is a standard technique used to test the performance and life cycle of the electrical storage devices including for the supercapacitors (Andrenacci et al., 2018). Capacitance can be plotted as a function of the cycle number, which is called the capacitance curve. Assuming a capacitor

exhibiting an ideal behavior, the capacitance of the capacitor (C) can be calculated based on Eq(2) and the slope of the curve, i.e.,  $dV / dt$  is a constant.

$$C = \frac{i}{\left(\frac{dV}{dt}\right)} \quad (2)$$

The increase in the self-discharge leads to the exponential shape of the charging and discharging voltage curves (Lewandowski et al., 2013). A higher equivalent serial resistance causes an increase in the high voltage drop in each cycle. The cycles were measured at 1, 100, 500, 1,000 and 1,500 cycles.

### 3. Results and discussions

#### 3.1 Capacitance measurement

The capacitance measurements were performed using the scan rate of 5, 10, 20, 40, 60, and 100  $\text{mV s}^{-1}$  with an electric potential range of -0.5 to 0.5 V. The capacitance was measured using the electrolyte variations, i.e., 10 %, 20 %, 30 % of  $\text{BaCO}_3$  or  $\text{CaCO}_3$ .

The cyclic voltammogram shows the relationship between the current changes and voltage at various scan rates across the electrodes. The curve shape of the carbon-based supercapacitor resembles a rectangle which was similar to that obtained by other author (Ahmed et al., 2018).

There is a significant shift of the potential window in the supercapacitor with  $\text{CaCO}_3$  electrolyte (Figure 2b) as the electrolyte concentration increases. This characteristic is not found in a supercapacitor with  $\text{BaCO}_3$  electrolyte (Figure 2a). This was due to the differences in the current generated by its potential range. The capacitance was calculated based on a voltammogram using formula (1). The calculation results are shown in Table 1.

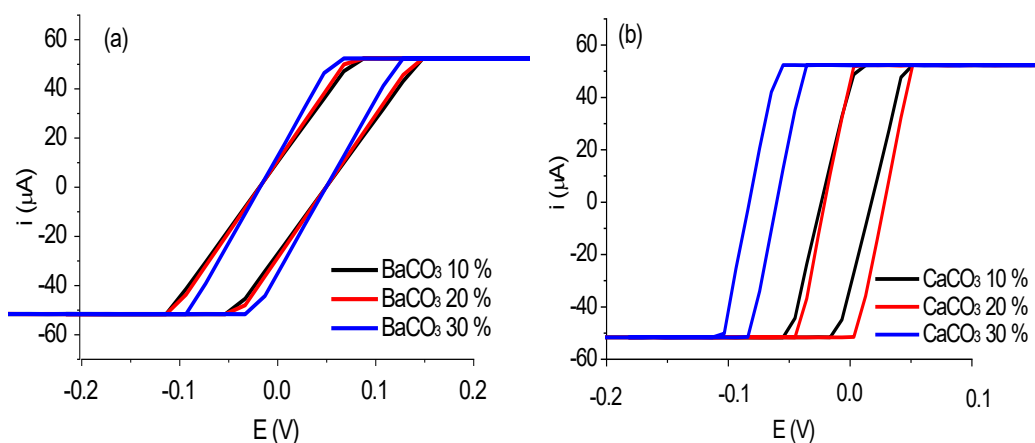


Figure 2: The voltammogram of the supercapacitors with electrolyte (a)  $\text{BaCO}_3$ ; and (b)  $\text{CaCO}_3$  at 20  $\text{mV s}^{-1}$  scan rate

Table 1: Capacitance of the supercapacitor using  $\text{BaCO}_3$  or  $\text{CaCO}_3$  as electrolyte

Scan rate ( $\text{mVs}^{-1}$ )	Capacitance ( $\text{mF} \cdot \text{g}^{-1}$ )			Capacitance of ( $\text{mF} \cdot \text{g}^{-1}$ )		
	$\text{BaCO}_3$ 10 %	$\text{BaCO}_3$ 20 %	$\text{BaCO}_3$ 30 %	$\text{CaCO}_3$ 10 %	$\text{CaCO}_3$ 20 %	$\text{CaCO}_3$ 30 %
5	2.81	2.98	4.80	5.54	5.31	2.37
10	2.38	2.61	4.17	4.09	3.76	1.96
20	3.91	4.15	6.24	6.95	6.16	3.31
40	3.12	3.50	5.48	5.47	4.64	2.92
60	3.46	3.65	5.46	5.96	5.04	2.98
100	3.63	4.26	4.63	5.62	4.67	3.20

Table 1 show that the highest capacitance value was achieved in the supercapacitor using 10 %  $\text{CaCO}_3$ , i.e., 6.95  $\text{mF g}^{-1}$ ; the capacitance value was 3.91  $\text{mF g}^{-1}$  for 10 %  $\text{BaCO}_3$ . The capacitance decreased with the increase of the scan rate. It is associated with the ion diffusion resistance in certain micro pores, as only a portion of the micro pores can be accessed by the electrolyte (Yang et al., 2017). This condition can be

clarified with a decrease in the electrolyte concentration at a high scan rate. At low concentrations, the dominant double layer occurs in the pores as mass displacements on the microstructure progress slowly (Ghosal et al., 2019).

At higher concentration of electrolyte, the mass transfer rate increased with the increasing concentration gradient and motion force as well as the reduced resistance friction. In different situation, the mass transfer in the double-layer of the supercapacitor could affects its voltage shift depending on the cyclic voltammetry (Figure 1). Barium ions make the electrical double layer formation much more stable than the calcium ion due to the differences of their ion size.

### 3.2 Stability of charging and discharging process in supercapacitor

Galvanostatic charging-discharging (GCD) is a widely used method for testing capacitances as the measurements can be easily connected with the load applied to supercapacitor (Kim et al., 2015). Figure 3 shows the measurements by galvanostatic. The GCD profile shows some characteristics associated with the supercapacitor application. Charging – discharging cycle is the important parameter to determine the practical application especially the lifetime usage and the rate of the process (Narayan et al., 2018).

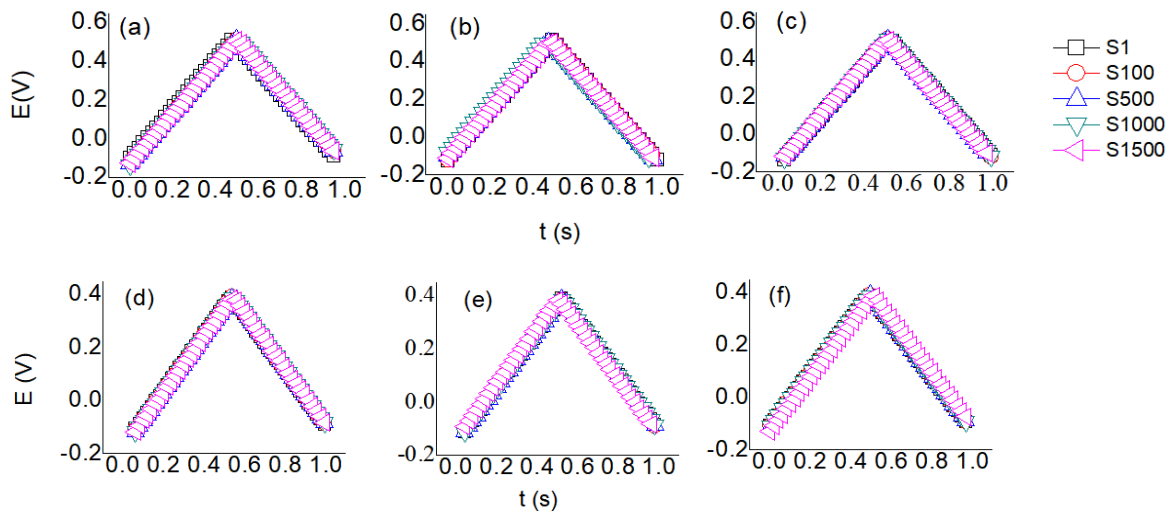


Figure 3: GCD profile of supercapacitor for the first cycle (s-1), 100th (s-100), 500th (s-500), 1,000th (s-1000) and 1,500th (s-1500) in BaCO<sub>3</sub> (a) 10 %, (b) 20 %, (c) 30 %; and in CaCO<sub>3</sub> (d) 10 %, (e) 20 %, (f) 30 %.

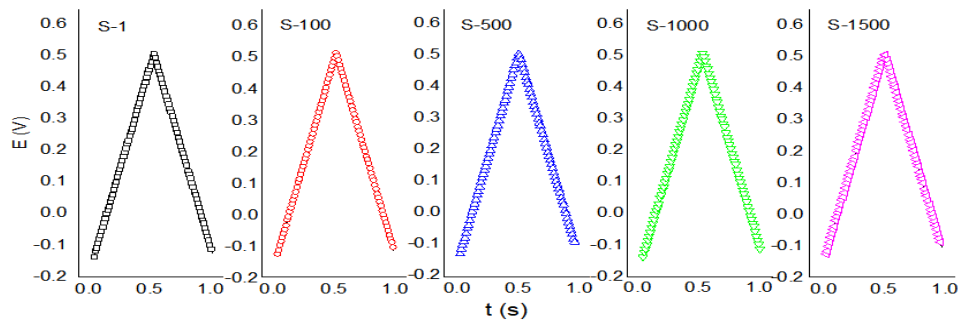


Figure 4: GCD profile of supercapacitor in polyvinyl alcohol for the 1<sup>st</sup> cycle (s-1), 100<sup>th</sup> (s-100), 500<sup>th</sup> (s-500), 1,000<sup>th</sup> (s-1000) and the 1,500<sup>th</sup> (s-1500) in 20 % CaCO<sub>3</sub>

The transition at the beginning of the cycle (1<sup>st</sup> and 100<sup>th</sup>) occurred when the supercapacitor was first in use, as shown in S-1 and S-100 cycles. The difference between the initial cycle and the next cycle was due to the arrangements of the distribution and dislocations on a molecular scale (Vatamanu et al., 2017). Such arrangements can be detected as a macro phenomenon in the expanding and shrinking of electrode matrices performed by the dilatometer equipment. The electrode will expand when charged and shrink when discharged. The supercapacitor shows a stable value in the cycles above 100<sup>th</sup>, then the charge and discharge calculations are performed at  $\geq 100^{\text{th}}$  cycle. After the 100<sup>th</sup> cycle, a steady state will be achieved,

and the supercapacitor will work fully thereafter. Based on the curve, the transition has to work fully in certain time and has tendency to decay after being used (Liu et al., 2016).

Figure 4 shows the sequence of the charging-discharging slope of the supercapacitor in several cycles. The test was conducted for 1<sup>st</sup>, 100<sup>th</sup>, 500<sup>th</sup>, 1,000<sup>th</sup> and 1,500<sup>th</sup> cycles of charging – discharging. There is only a slight decrease in the first cycle, as shown by the increasing slope. The first cycle plot (Figure 4 (a)) shows the existence of linearity both in the direction of charging and discharging. It shows that limited penetration of electrolyte into the electrode pores is limited by the high concentrations of electrolytes. The penetration ability varies depending on the size of the electrolyte ions used. The electrolyte variation causes significant changes either at the charging or discharging rate.

### 3.3 Charging and discharging

The slope values in the 100<sup>th</sup> of charging-discharging cycles are given in Table 2 and 3. Almost all supercapacitors showed the same slope values, meaning that the supercapacitors have the same rate in both the charging and discharging process.

Table 2: Charging and discharging slope in the 100<sup>th</sup> cycle of supercapacitor galvanostatic test

Electrolyte of supercapacitor	Slope	
	Charging	Discharging
BaCO <sub>3</sub> 10 %	0.367	-0.367
BaCO <sub>3</sub> 20 %	0.894	-0.957
BaCO <sub>3</sub> 30 %	1.330	-1.330
CaCO <sub>3</sub> 10 %	0,916	-0,916
CaCO <sub>3</sub> 20 %	1,345	-1,344
CaCO <sub>3</sub> 30 %	0,889	-0,889

Table 3: Charging and discharging slope of different cycle in 20 % CaCO<sub>3</sub> of supercapacitor galvanostatic test

Cycle	Slope	
	Charging	Discharging
1 <sup>st</sup>	1.050	-1.050
100 <sup>th</sup>	1.345	-1.344
500 <sup>th</sup>	1.343	-1.245
1,000 <sup>th</sup>	1,344	-1,244
1,500 <sup>th</sup>	1.343	-1.244

Only the supercapacitor using 20 % CaCO<sub>3</sub> has a different slope value for its charging and discharging rate, i.e., 1.345 and -1.344. This result indicated that the supercapacitor has a faster charging rate than its discharging rate. Only the supercapacitor with 20 % CaCO<sub>3</sub> electrolyte has achieved the desired value regarding the standard requirement of a supercapacitor (Table 2). There is a complex (non-linear) relationship between the electrolytes and the capacitance, also between the electrolytes and the voltage of the supercapacitor (Li et al., 2018). It can be seen from Table 3 that the slopes, both for charging and discharging, where the supercapacitor has stability in charging and discharging process as shown by the slope.

These results highlight the capability of the electrode preparation method and the use of polymer based electrolyte to produce supercapacitor with acceptable capacitance value, that is 1.96 to 6,98 mF for supercapacitor having the size of 190 mm x 30 mm x 1 mm with reasonable charging -discharging rate. The supercapacitor using CaCO<sub>3</sub> electrolyte has the best capacitance.

## 4. Conclusions

A supercapacitor made of the novel carbon nanosheets derived from the aquatic wood waste was developed. The result of the cyclic voltammetry tests showed that the highest value of supercapacitor was achieved using 10 % of CaCO<sub>3</sub> electrolyte, i.e., 6.95 mFg<sup>-1</sup>, as compared to only 3.91 mFg<sup>-1</sup> using 10 % BaCO<sub>3</sub>. Most of the supercapacitors have the same slope value indicating that they have the same rate in both the charging and discharging process. Except for the supercapacitor using 20 % CaCO<sub>3</sub>, a different slope was obtained where the supercapacitor has a charging rate faster than its discharging rate. In order to produce a supercapacitor that meets these two requirements, future study will improve the current collection section that contacts the

two electrodes. The energy storage made from the novel carbon nanosheets show capacitance values that are appropriate for their category as a supercapacitor.

### Acknowledgments

The financial support for this research was provided by Universitas Sriwijaya. LPPM Universitas Sriwijaya is gratefully acknowledged for the award of 'hibah kompetitif' and 'hibah profesi' grant.

### References

- Ahmed S., Ahmed A., Rafat M., 2018, Supercapacitor performance of activated carbon derived from rotten carrot in aqueous, organic and ionic liquid based electrolytes, *Journal of Saudi Chemical Society*, 22, 993–1002.
- Allagui A., Freeborn T.J., Elwakil A.S., Maundy B.J., 2016, Reevaluation of Performance of Electric Double-layer Capacitors from Constant-current Charge/Discharge and Cyclic Voltammetry, *Scientific Reports*, 6, 38568.
- Andrenacci N., Chiodo E., Lauria D., Mottola F., 2018, Life cycle estimation of battery energy storage systems for primary frequency regulation, *Energies*, 11, 3320.
- Correa C., Kruse A., 2018, Biobased functional carbon materials: Production, characterization, and applications—A review, *Materials*, 11, 1568.
- Fic K., Platek A., Piwek J., Frackowiak E., 2018, Sustainable materials for electrochemical capacitors, *Materials Today*, 21, 437–454.
- Ghosal S., Sherwood J.D., Chang H.-C., 2019, Solid-state nanopore hydrodynamics and transport, *Biomicrofluidics*, 13, 011301.
- Iro Z.S., Subramani C., Dash C.C., 2016, A brief review on electrode materials for supercapacitor, *International Journal of Electrochemical Science*, 11, 10628–10643.
- Kim B.K., Sy S., Yu A., Zhang J., 2015, Electrochemical Supercapacitors for Energy Storage and Conversion, *Handbook of Clean Energy Systems*. John Wiley & Sons, Ltd, Chichester, UK, 1–25.
- Lewandowski A., Jakobczyk P., Galinski M., Biegun M., 2013, Self-discharge of electrochemical double layer capacitors, *Physical Chemistry Chemical Physics*, 15, 8692.
- Li Z., Jeanmairet G., Mendez-Morales T., Rotenberg B., Salanne M., 2018, Capacitive performance of water-in-salt electrolyte in supercapacitors: A simulation study, *Journal of Physical Chemistry*, 122, 23917 – 23924.
- Liu C., Neale Z.G., Cao G., 2016, Understanding electrochemical potentials of cathode materials in rechargeable batteries, *Materials Today*, 19, 109–123.
- Narayan N., Papakosta T., Vega-Garita V., Qin Z., Popovic-Gerber J., Bauer P., Zeman M., 2018, Estimating battery lifetimes in Solar Home System design using a practical modelling methodology, *Applied Energy*, 228, 1629–1639.
- Giudicianni P., Pindozi S., Grottola C.M., Stanzione F., Faugno S., Fagnano M., Fiorentino N., Ragucci R., 2017, Effect of feedstock and temperature on the distribution of heavy metals in char from slow steam pyrolysis of contaminated biomasses, *Chemical Engineering Transactions*, 58, 505–510.
- Syabania N.F., Sudarsono W., Rohendi D., Syarif N., 2018, Functionality analysis of carbon nanosheet, oxidized carbon nanosheet and reduced carbon nanosheet oxide by using fourier transform infrared and Boehm titration method, *Journal of Physics: Conference Series*, 1095, 012028.
- Syarif N., Pardede M.C., 2014, Hydrothermal assisted microwave pyrolysis of water hyacinth for electrochemical capacitors electrodes, *International Transaction Journal of Engineering, Management & Applied*, 5, 95–101.
- Syarif N., Prasagi M., 2016, Preparation of carbon nanosheets from Gelam wood bark and its electrochemical study, *Carbon – Science and Technology*, 8, 35–42.
- Vatamanu J., Borodin O., Olguin M., Yushin G., Bedrov D., 2017, Charge storage at the nanoscale: understanding the trends from the molecular scale perspective, *Journal of Materials Chemistry A*, 5, 21049–21076.
- Yang I., Kim S.-G., Kwon S.H., Kim M.-S., Jung J.C., 2017, Relationships between pore size and charge transfer resistance of carbon aerogels for organic electric double-layer capacitor electrodes, *Electrochimica Acta*, 223, 21–30.
- Zhi J., Cui H., Wang Z., Huang F., 2018, Surface confined titania redox couple for ultrafast energy storage, *Materials Horizons*, 5, 691–698.